AMERICAN SOCIETY FOR MICROBIOLOGY | Journal of Bacteriology®

RESEARCH ARTICLE

Regulatory Properties of the ADP-Glucose Pyrophosphorylase from the Clostridial *Firmicutes* Member *Ruminococcus albus*

Antonela E. Cereijo,[a] Matías D. Asencion Diez,[a,b] Miguel A. Ballicora,[b] Alberto A. Iglesias[a]

[a]Instituto de Agrobiotecnología del Litoral (UNL-CONICET), Facultad de Bioquímica y Ciencias Biológicas, Santa Fe, Argentina

[b]Department of Chemistry and Biochemistry, Chicago, Illinois, USA

ABSTRACT ADP-glucose pyrophosphorylase from *Firmicutes* is encoded by two genes (*glgC* and *glgD*) leading to a heterotetrameric protein structure, unlike those in other bacterial phyla. The enzymes from two groups of *Firmicutes*, *Bacillales* and *Lactobacillales*, present dissimilar kinetic and regulatory properties. Nevertheless, no ADP-glucose pyrophosphorylase from *Clostridiales*, the third group in *Firmicutes*, has been characterized. For this reason, we cloned the *glg*C and *glg*D genes from *Ruminococcus albus*. Different quaternary forms of the enzyme (GlgC, GlgD, and GlgC/GlgD) were purified to homogeneity and their kinetic parameters were analyzed. We observed that GlgD is an inactive monomer when expressed alone but increased the catalytic efficiency of the heterotetramer (GlgC/GlgD) compared to the homotetramer (GlgC). The heterotetramer is regulated by fructose-1,6-bisphosphate, phosphoenolpyruvate, and NAD(P)H. The first characterization of the *Bacillales* enzyme suggested that heterotetrameric ADP-glucose pyrophosphorylases from *Firmicutes* were unregulated. Our results, together with data from *Lactobacillales*, indicate that heterotetrameric *Firmicutes* enzymes are mostly regulated. Thus, the ADP-glucose pyrophosphorylase from *Bacillales* seems to have distinctive insensitivity to regulation.

IMPORTANCE The enzymes involved in glycogen synthesis from *Firmicutes* have been less characterized in comparison with other bacterial groups. We performed kinetic and regulatory characterization of the ADP-glucose pyrophosphorylase from *Ruminococcus albus*. Our results showed that this protein that belongs to different groups from *Firmicutes* (*Bacillales*, *Lactobacillales*, and *Clostridiales*) presents dissimilar features. This study contributes to the understanding of how this critical enzyme for glycogen biosynthesis is regulated in the *Firmicutes* group, whereby we propose that these heterotetrameric enzymes, with the exception of *Bacillales*, are allosterically regulated. Our results provide a better understanding of the evolutionary relationship of this enzyme family in *Firmicutes*.

KEYWORDS glycogen, GlgC, GlgD, allosterism, ADP-glucose pyrophosphorylase, *Ruminococcus albus*, fructose-1,6-bisphosphate, glycogen metabolism, phosphoenolpyruvate, pyruvate

Glycogen is a polysaccharide formed by glucose (Glc) units linked by α-1,4 bonds arranging a main chain with α-1,6 ramifications. Although the polymer meets the criteria for a storage compound and has been isolated from more than 50 different bacterial species, its precise role in prokaryotes is still poorly understood (1, 2). Bacterial glycogen synthesis from glucose-1-phosphate (Glc-1P) is performed by three steps, in which the key metabolite ADP-Glc is the specific glucosyl donor (2–4). The limiting step in the pathway is at the level of ADP-Glc biosynthesis catalyzed by ADP-Glc pyrophos-

Received 29 March 2018 **Accepted** 19 June 2018

Accepted manuscript posted online 25 June 2018

Citation Cereijo AE, Asencion Diez MD, Ballicora MA, Iglesias AA. 2018. Regulatory properties of the ADP-glucose pyrophosphorylase from the clostridial *Firmicutes* member *Ruminococcus albus*. J Bacteriol 200:e00172-18. https://doi.org/10.1128/JB.00172-18.

Editor William W. Metcalf, University of Illinois at Urbana Champaign

Address correspondence to Alberto A. Iglesias, iglesias@fbcb.unl.edu.ar.

phorylase (ADP-Glc PPase; EC 2.7.7.27), an allosteric enzyme regulated by metabolites from the main carbon utilization route(s) in the organism (2–4).

ADP-Glc PPases from prokaryotes were classified according to their structural and regulatory properties into eight different classes (3, 4). The enzyme from *Bacillus* spp. was a distinctive case because of its heterotetrameric structure and insensitivity to allosteric effectors. All other bacterial forms characterized before had been homotetrameric and regulated (2, 3, 5–7). At that time, the enzyme from *Bacillus* spp. was the only one reported from a Gram-positive bacterium (3, 4). Recently, our group characterized different ADP-Glc PPases from Gram-positive bacteria to get a deeper understanding on the functional evolution of this enzyme family (8–11). Enzyme forms from non-*Firmicutes* (high G+C content) Gram-positive bacteria are highly regulated homotetramers (10, 11). Low-G+C-content Gram-positive (*Firmicutes*) genomes show the occurrence of two distinct genes, *glgC* and *glgD*, coding for ADP-Glc PPase (8). In two groups of *Firmicutes* (*Bacillales* and *Lactobacillales*) the enzyme is composed of a catalytic subunit (GlgC) and a noncatalytic subunit (GlgD) (3, 7, 8).

Biochemical properties of enzymes involved in glycogen metabolism in *Firmicutes* have not been completely characterized. Only two ADP-Glc PPases from this group of bacteria, those from *Geobacillus stearothermophilus* (7) and *Streptococcus mutans* (8, 12), have been studied. The former was insensitive to allosteric effectors, with minor kinetic differences between the homotetrameric (GlgC) and the heterotetrameric (GlgC/GlgD) forms (7). On the other hand, the kinetic and regulatory properties of the *S. mutans* ADP-Glc PPase markedly differ from those of the *G. stearothermophilus* enzyme. The heterotetrameric GlgC/GlgD from *S. mutans* was found to be 1 order of magnitude more active than the homotetrameric GlgC, with significant differences regarding affinity toward substrates (8). In addition, fructose-1,6-bisphosphate (Fru-1,6-P_2) activated GlgC but had no effect on GlgC/GlgD, while phosphoenolpyruvate (PEP) and inorganic orthophosphate (P_i) inhibited GlgC/GlgD without affecting GlgC.

To further understand the properties of *Firmicutes* ADP-Glc PPases clustered in different phylogenetic groups, we conducted molecular cloning of the *glg*C and *glg*D genes encoding the enzyme in the clostridial bacterium *Ruminococcus albus*. The recombinant GlgC, GlgD, and GlgC/GlgD forms were highly purified and functionally characterized. Results indicate distinctive kinetic and regulatory properties for the *R. albus* ADP-Glc PPase as hypothesized from phylogenetic classification.

RESULTS

Functionality of the *R. albus* ADP-Glc PPase. *R. albus* belongs to the family *Ruminococcaceae* from the order *Clostridiales* in the *Firmicutes* phylum (13). An *in silico* analysis of the *R. albus* genome (14) showed the presence of the *glgC* and *glgD* genes encoding ADP-Glc PPase, as in the other two orders from *Firmicutes* (7, 8). The *R. albus* GlgC (*RalglgC* product) and GlgD (*RalglgD* product) proteins have 24.1% identity. The *RalglgC* gene (1,203 bp) encodes a 44.5-kDa protein that has ~50% identity with their GlgC homologues from *S. mutans* and *G. stearothermophilus* (7, 8). The GlgD subunit is a 41.6-kDa protein sharing 24% and 33% identity with the GlgD proteins from *S. mutans* and *G. stearothermophilus*, respectively. To shed light on the structure-function relationship of this enzyme from the *Clostridiales* order, we cloned both the *RalglgC* and *RalglgD* genes to produce the *R. albus* ADP-Glc PPase in different expression systems.

To analyze functionality, we used the pMAB5/*RalglgC* and pMAB6/*RalglgD* constructs, respectively, expressing GlgC and GlgD proteins in *Escherichia coli* AC70R1-504 cells, which is a system used before for heterotetrameric ADP-Glc PPases (8, 15). The activity in crude extracts from cells expressing *R. albus* GlgC protein was at least 800-fold higher than for nontransformed cells (Fig. 1A) (basal activity, 0.03 ± 0.01 mU/mg). On the other hand, cells expressing GlgD alone had values of activity that were not significantly different from those of nontransformed cells. This suggests that *R. albus* GlgD by itself is unable to catalyze ADP-Glc formation. In addition, extracts coexpressing both GlgC/GlgD subunits were 1.7-fold more active than those expressing GlgC alone. This indicates that there is a synergic effect between the *R. albus* ADP-Glc

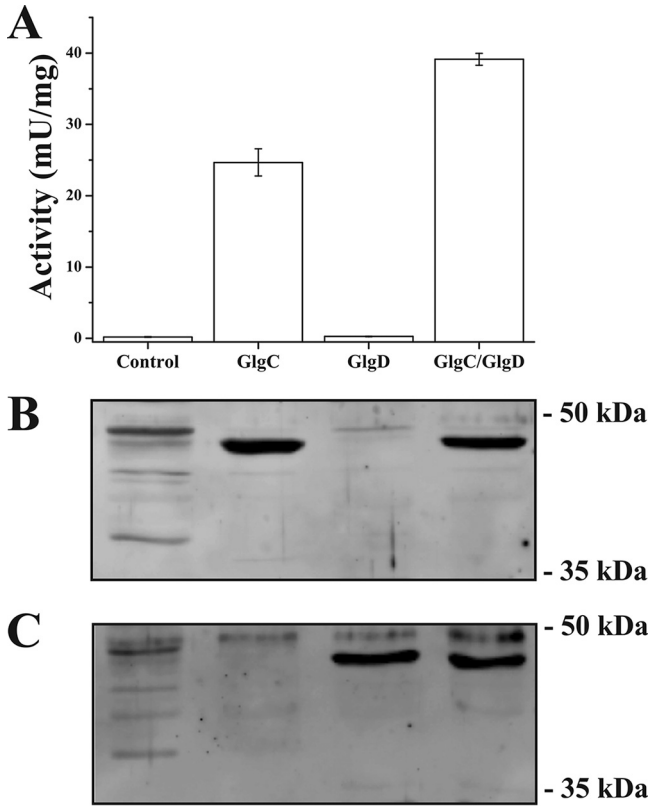

FIG 1 Expression of genes coding for *R. albus* ADP-Glc PPase in *E. coli* AC70R1-504 cells. (A) Specific ADP-Glc PPase activity in crude extracts of cells transformed with the following plasmids: none (control), pMAB5/*RalglgC* (GlgC), pMAB6/*RalglgD* (GlgD), and pMAB5/*RalglgC* plus pMAB6/*RalglgD* (GlgC/GlgD). The basal activity was 0.03 ± 0.01 mU/mg. (B and C) Immunodetection of the *R. albus* ADP-Glc PPase subunits in soluble crude extracts, stained using as primary antibodies those raised against the *G. stearothermophilus* GlgC and GlgD subunits.

PPase subunits. Immunoassays confirmed the presence of GlgC, GlgD, or GlgC/GlgD in the respective crude extracts (Fig. 1B and C). Together, the results indicate that GlgC is catalytic *per se*, whereas GlgD is inactive. GlgD would be regulatory by enhancing the activity of GlgC.

For a comparative functional analysis of the different oligomeric forms of the ADP-Glc PPase, we used an *in vivo* system. We took advantage of the *E. coli* AC70R1-504 strain deficiency in ADP-Glc PPase activity and its consequent impaired capacity to accumulate glycogen (5). Transformed cells expressing GlgC, GlgD, or GlgC/GlgD from *R. albus*, *S. mutans* or *G. stearothermophilus* were grown and analyzed regarding polysaccharide accumulation. As shown in Fig. 2, glycogen accumulation was clearly detected in pellets from cells expressing the *R. albus* GlgC or GlgC/GlgD forms but not in cells expressing the GlgD subunit alone. Moreover, we observed a higher glycogen accumulation for *R. albus* GlgC/GlgD than for GlgC. This is in good agreement with the enzyme assays from crude extracts (Fig. 1A) indicating that both GlgC and GlgC/GlgD conformations are the active *R. albus* ADP-Glc PPase structures.

Glycogen accumulation in cells bearing *S. mutans* and *G. stearothermophilus* ADP-Glc PPases followed a pattern similar to that of cells transformed with *R. albus* forms. Iodine staining assays for cells producing *S. mutans* enzymes show that heteromeric GlgC/GlgD exhibited a strong dark brown color compared to brownish pellets from the GlgC expression (Fig. 2A). As well, strong dark brown pellets with no difference between GlgC and GlgC/GlgD were obtained for the *G. stearothermophilus* enzyme. No staining was detected in pellets from cells expressing the GlgD subunit alone from either *S. mutans* or *G. stearothermophilus*. These results agree with the previous reports showing

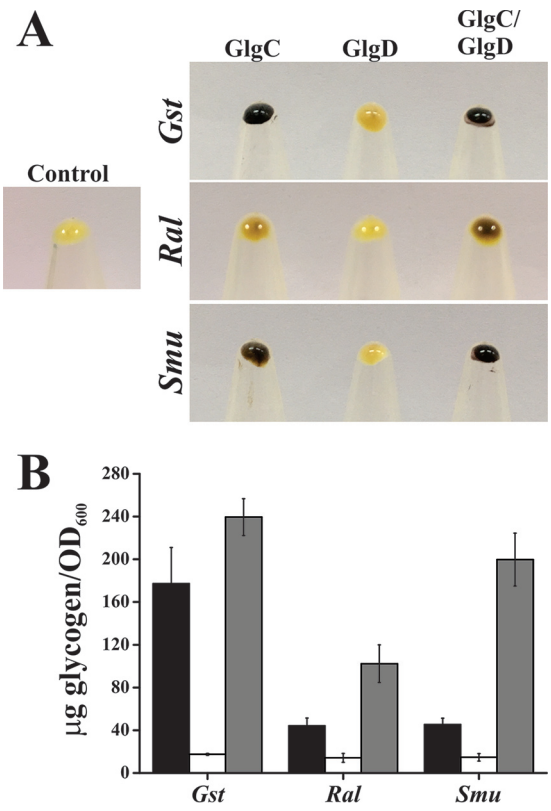

FIG 2 Functionality of the genes coding for the *R. albus* ADP-Glc PPase. (A) Iodine staining of cell pellets from *E. coli* AC70R1-504: nontransformed (control) or transformed to produce GlgC, GlgD, or GlgC/GlgD proteins from *G. stearothermophilus* (*Gst*), *R. albus* (*Ral*), or *S. mutans* (*Smu*). (B) Glycogen accumulation in extracts from cells transformed with *glgC* (black bars), *glgD* (white bars), or *glgC/glgD* (gray bars) genes. Glycogen accumulation in control cells was 13.65 ± 0.01 μg of glycogen/OD_{600}. For *S. mutans* ADP-Glc PPase production, cells were transformed with pMAB6/*SmuglgC* and pMAB5/*SmuglgD* vectors as described previously (8).

that *S. mutans* GlgC/GlgD had 10-fold more activity than GlgC and that both homo- and heteromeric *G. stearothermophilus* structures had similar activities (7, 8). All the results from Fig. 2A were confirmed by the quantitative glycogen accumulation determination shown in Fig. 2B. Results suggest that the *Clostridiales R. albus* enzyme may reach intermediate level of activity *in vivo* compared with *Bacillales* and *Lactobacillales* ADP-Glc PPases.

Kinetic characterization of recombinant GlgC, GlgD, and GlgC/GlgD from *R. albus*. The *R. albus glgC* and *glgD* genes were expressed separately or together using the pET/pDUET systems to produce recombinant proteins with or without His tags. Higher purity levels (>80%) were obtained with an N-terminally fused His tag, and purities between 50 and 80% were obtained when no tag was included (see Fig. S1 in the supplemental material). We determined that for *R. albus* ADP-Glc PPase the forms with and without the tag exhibited similar kinetic behaviors (data not shown). Thus, we report results from His-tagged proteins. Specific activities of purified GlgC and GlgC/GlgD were 0.85 U/mg and 2.10 U/mg, respectively, whereas the activity of the GlgD subunit (also highly purified) was negligible ($<5 \times 10^{-4}$ U/mg). Quaternary structures for *R. albus* GlgC, GlgD, and GlgC/GlgD were determined by size exclusion chromatography, as shown in Fig. S1B in the supplemental material. Both GlgC and GlgC/GlgD behaved as tetrameric proteins, with molecular masses of 180 kDa and 173 kDa, respectively. This is in agreement with ADP-Glc PPases in general and with the *G. stearothermophilus* and *S. mutans* enzymes, which are also encoded by the *glgC* and *glgD* genes (7, 8). The GlgD protein was eluted as a monomer (Fig. S1B), as was reported for *G. stearothermophilus* GlgD (7).

TABLE 1 Kinetic parameters of the *R. albus* ADP-Glc PPase forms in the absence and in the presence of allosteric activators

Effector and parameter	Value for protein			
	GlgC		GlgC/GlgD	
	Glc-1P	ATP	Glc-1P	ATP
None				
$S_{0.5}$ (mM)	0.45 ± 0.03	1.50 ± 0.09	0.27 ± 0.02	0.69 ± 0.04
n_H	0.9	1.4	0.7	1.6
V_{max} (U/mg)	0.87 ± 0.01	0.87 ± 0.01	2.1 ± 0.1	2.1 ± 0.1
Pyr (50 mM)				
$S_{0.5}$ (mM)	0.41 ± 0.06	1.2 ± 0.1	No activation	No activation
n_H	1.0	2.0	No activation	No activation
V_{max} (U/mg)	1.14 ± 0.05	1.14 ± 0.05	No activation	No activation
PEP (12 mM)				
$S_{0.5}$ (mM)	0.73 ± 0.05	1.15 ± 0.05	0.16 ± 0.01	0.77 ± 0.09
n_H	1.0	1.3	1.2	1.0
V_{max} (U/mg)	1.85 ± 0.05	1.85 ± 0.05	5.8 ± 0.2	5.8 ± 0.2
Fru-1,6-P_2 (12 mM)				
$S_{0.5}$ (mM)	0.44 ± 0.04	1.4 ± 0.1	1.82 ± 0.09	1.7 ± 0.2
n_H	0.7	0.9	0.7	2.8
V_{max} (U/mg)	0.31 ± 0.01	0.31 ± 0.01	1.35 ± 0.01	1.35 ± 0.01
NADH (5 mM)				
$S_{0.5}$ (mM)			1.2 ± 0.1	2.5 ± 0.2
n_H			0.9	2.4
V_{max} (U/mg)			2.1 ± 0.2	2.1 ± 0.2

The GlgC and GlgC/GlgD forms of the *R. albus* ADP-Glc PPase were characterized in the synthesis of ADP-Glc direction. Saturation curves for Glc-1P and ATP were near hyperbolic for both forms of the *R. albus* enzyme. The heterotetrameric GlgC/GlgD displayed a 2.4-fold-higher V_{max} than that determined for the homotetrameric GlgC (Table 1). As well, *R. albus* GlgC/GlgD had higher apparent affinities for both ATP (2.2-fold) and Glc-1P (1.7-fold) substrates. The different kinetic properties between GlgC/GlgD and GlgC suggest that GlgD has an activating role in the heterotetramer. Taken together, the kinetic properties of the *R. albus* ADP-Glc PPase resemble those of the *S. mutans* (8) rather than the *G. stearothermophilus* (7) homologous enzyme, if compared to the ADP-Glc PPases from *Firmicutes* studied to date.

Regulatory properties of *R. albus* GlgC and GlgC/GlgD. ADP-Glc PPase from the *Bacillales* group of *Firmicutes* was the only bacterial form reported to be insensitive to regulation (6, 7). To see if the enzyme from the *Clostridiales* group is regulated, we assayed the *R. albus* forms in the presence of different metabolites known to modulate the ADP-Glc PPase activity from different sources (3, 8, 10, 11). Assays were performed using two sets of Glc-1P and ATP concentrations: subsaturating (concentration near the respective value for 50% of the maximal velocity [$S_{0.5}$]) or saturating (concentration around 3-fold higher than the respective $S_{0.5}$ value) conditions with respect to substrates. Of the several compounds analyzed, Pyr, PEP, Fru-1,6-P_2, NADH, and NADPH were those that exerted effect on the activity of the enzymes (Table S1 in the supplemental material). The effects of Pyr, PEP, and Fru-1,6-P_2 were independent of substrate concentration, while NADH and NADPH only affected activity assayed at subsaturating levels of Glc-1P and ATP. A different property of the *R. albus* enzymes in comparison with GlgC and GlgC/GlgD of *S. mutans* (8) is that under either subsaturating or saturating levels of substrates, no effect by high concentrations (up to 500 mM) of the salts $MgSO_4$, KCl, NaCl, and NH_4Cl was observed (data not shown).

Pyr specifically activated GlgC, with no effect on GlgC/GlgD (even when assayed up to 50 mM) (Fig. 3A). The keto acid increased 1.6-fold the *R. albus* GlgC maximum rate of metabolism (V_{max}) (Table 1), with an activator concentration giving a value for 50%

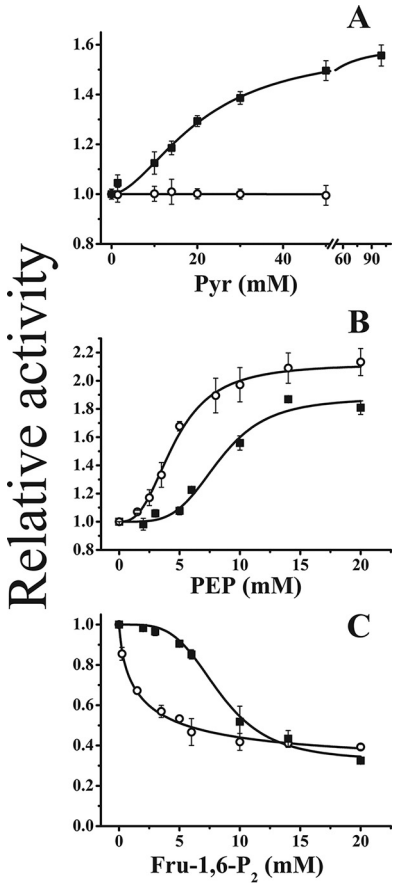

FIG 3 Sensitivity to allosteric regulators of active structures of *R. albus* ADP-Glc PPase. Responses of GlgC/GlgD (open symbols) and GlgC (filled symbols) to different concentrations of Pyr (A), PEP (B), and Fru-1,6-P_2 (C) are depicted. Values of relative activity were calculated as the ratio of activity determined at each specific condition related to the activity of the respective enzyme form assayed in the absence of effector: 0.87 ± 0.01 U/mg for GlgC and 2.1 ± 0.1 U/mg for GlgC/GlgD.

of the maximal activation ($A_{0.5}$) of 20 ± 1 mM (Fig. 4A) and a Hill coefficient (n_H) of 1.8. PEP activated 1.9-fold ($A_{0.5}$ of 8.3 ± 0.7 mM; n_H of 4.1) and 2.1-fold ($A_{0.5}$ of 4.6 ± 0.2 mM; n_H of 2.7), respectively, *R. albus* GlgC and GlgC/GlgD (Fig. 3B and Table 1). On the other hand, Fru-1,6-P_2 was previously described as an activator of ADP-Glc PPases in same species (including the *S. mutans* GlgC enzyme) (1, 3, 8). However, it behaved as an inhibitor of both oligomeric forms of the *R. albus* enzyme (Fig. 3C). Both structures were inhibited to 40% of activity but with dissimilar kinetic behaviors. GlgC/GlgD inhibition by Fru-1,6-P_2 had an inhibitor concentration giving 50% of the maximal inhibition ($I_{0.5}$) of 1.9 ± 0.1 mM (n_H of 0.7), whereas the inhibition of GlgC was highly sigmoidal, with an $I_{0.5}$ of 8.3 ± 0.4 mM (n_H of 3.9). Interestingly, GlgD had a significant effect on the sigmoidicity of the ATP saturation curve in the presence of inhibitors (Table 1), nullifying the activation effect of Pyr. This suggests that GlgD makes the enzyme more sensitive to ATP concentrations when inhibitors are present. It is important to take into account that variations of intracellular levels of ATP are clear signals of energy available.

Figure 4 details the effect of NAD(P)H (and the respective oxidized forms) on the activities of the *R. albus* enzymes. $NAD(P)^+$ had no effect or slightly activated the GlgC and GlgC/GlgD enzymes. On the other hand, inhibition exerted by NADH followed hyperbolic patterns, with $I_{0.5}$ values calculated at 1 mM for GlgC and 3 mM for GlgC/GlgD. NAPDH inhibition was less effective, with sigmoid saturation curves and $I_{0.5}$ values of 5 mM and 10 mM for GlgC and GlgC/GlgD, respectively. The results suggest that under the cellular condition of *R. albus* the activity of ADP-Glc PPase would be

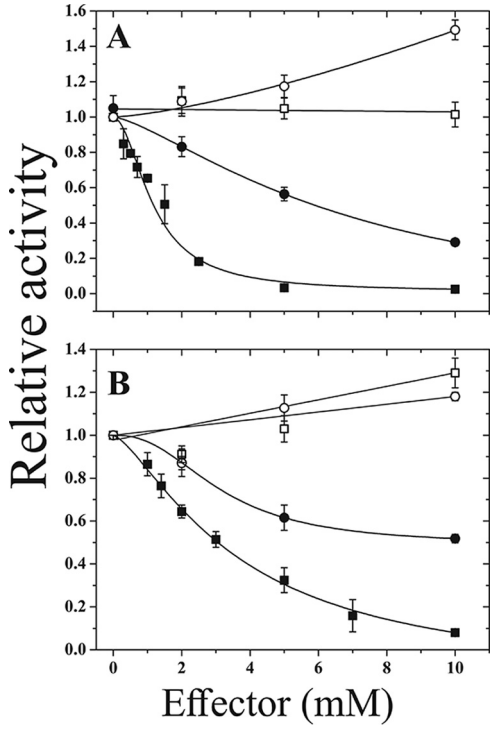

FIG 4 Inhibitory effect of NAD(P)H in *R. albus* ADP-Glc PPase GlgC (A) and GlgC/GlgD (B) conformations. Inhibition curves were determined at subsaturating substrate concentrations. The value 1 equals 0.11 U/mg and 0.38 U/mg for GlgC or GlgC/GlgD, respectively. Filled symbols correspond to NADH (■) and NADPH (●), while empty symbols correspond to NAD^+ (□) and $NADP^+$ (○).

modified depending on the ratio $NAD(P)^+$ to NAD(P)H, inhibiting the enzyme under more reducing environments.

We further explored the regulation of the *R. albus* ADP-Glc PPase forms by analyzing changes produced by the effectors on the substrate kinetics, determining the enzyme catalytic efficiency ratio $V_{max}/S_{0.5}$; equivalent to k_{cat}/K_m for hyperbolic kinetics (11, 16–18) for comparative analysis. As detailed in Table 1, allosteric effectors modified V_{max} and/or $S_{0.5}$ values to different extents. Particularly, Pyr and PEP increased the GlgC catalytic efficiency, while Fru-1,6-P_2 and NADH produced the opposite effect (Fig. 5). GlgC catalytic efficiency increased up to ~2- or ~3-fold in the presence of Pyr or PEP, respectively, and it decreased ~2-fold in the presence of Fru-1,6-P_2 (Fig. 5). On the other hand, GlgC/GlgD was insensitive to Pyr. The main change in catalytic efficiency for Glc-1P was observed with GlgC/GlgD, since it was enhanced 5-fold by PEP and decreased 1 order of magnitude by Fru-1,6-P_2. As shown in Fig. S2 in the supplemental material, NADH decreased the apparent affinity of GlgC/GlgD toward ATP ($S_{0.5}$ of 2.5 ± 0.2 mM), with a more pronounced sigmoidal behavior (n_H of 2.1), but without affecting V_{max}. This resulted in a decrease of the catalytic efficiency of the enzyme that was near 5-fold. Such an inhibitory effect would be a typical K-type inhibitor that follows the Monod-Wyman-Changeux model of allosterism (19). In those cases, the inhibitor decreases the apparent affinity for the substrate and increases the sigmoidicity of the substrate (ATP) saturation curve (Table 1 and Fig. 4; see also Fig. S2 in the supplemental material).

Previous works showed the interaction between activators and inhibitors of the prokaryotic ADP-Glc PPase (8, 11, 16, 20, 21). Thus, we analyzed the activity of the *R. albus* GlgC/GlgD enzyme in the presence of saturating and nonsaturating concentrations of its effectors (shown in Fig. S3 in the supplemental material). The inhibition by Fru-1,6-P_2 was affected by different concentrations of PEP. Fru-1,6-P_2 can only inhibit the enzyme if PEP is not saturating (see Fig. S3A). On the other hand, the apparent affinity for PEP seems to be reduced by increasing concentrations of Fru-1,6-P_2 (Fig. S3B).

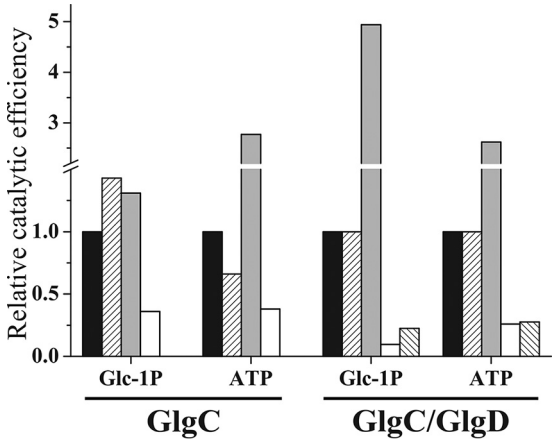

FIG 5 Relative catalytic efficiency of *R. albus* GlgC and GlgC/GlgD in the absence (black bars) or in the presence of 50 mM Pyr (right diagonal bars), 12 mM PEP (gray bars), 12 mM Fru-1,6-P_2 (white bars), and 5 mM NADH (left diagonal bars) for GlgC/GlgD. Relative catalytic efficiency was established as the ratio between the catalytic efficiency ($k_{cat}/S_{0.5}$) obtained under each condition and that, respectively, determined in the absence of effector for GlgC (5.80 s^{-1} mM^{-1} and 1.74 s^{-1} mM^{-1} for Glc-1P and ATP, respectively) and GlgC/GlgD (22.4 s^{-1} mM^{-1} and 8.77 s^{-1} mM^{-1} for Glc-1P and ATP, respectively).

DISCUSSION

Ruminococcus spp. are anaerobic bacteria that inhabit the rumen in cattle, sheep, and goats. These microorganisms are cellulolytic bacteria with an important role in fiber breakdown in the rumen, producing acetate, ethanol, formate, hydrogen, and carbon dioxide from carbohydrates. They are also capable of fermenting glucose and xylose (14, 22–25). Hydrogen-producing *R. albus* is abundant in the gut microbiota in healthy individuals (26), showing probiotic effects (25) with a potential neuroprotective action (27). *R. albus* belongs to the *Clostridiales*, one of the groups in the phylum *Firmicutes* together with *Bacillales* and *Lactobacillales* (13, 28). Previously, it was demonstrated that glycogen accumulates in *Clostridium cellulolyticum* (belonging to the *Clostridiales*) reactors fed with cellobiose during different stages of growth (29). In addition, it was reported that *R. albus* accumulates a glycogen-like polysaccharide in late log and early stationary phases (30), although no enzymatic pathway was described for the polyglucan synthesis in this bacterium. Here we present the first kinetic, regulatory, and structural characterization of an enzyme related to glycogen metabolism in *Clostridiales*.

In previous studies (7, 8), ADP-Glc PPases from *Bacillales* and *Lactobacillales* showed dissimilar kinetic and regulatory properties. The one from *Bacillales* was the only unregulated one known to that point (7), and the one from *Lactobacillales* showed a fine-tuned regulation (8). In this study, the homo- and heterotetrameric forms of the *R. albus* ADP-Glc PPase displayed different properties from the *G. stearothermophilus* and *S. mutans* enzymes. The homotetrameric *R. albus* GlgC had a catalytic efficiency 10-fold lower than that of the *G. stearothermophilus* GlgC and 10-fold higher than that of the *S. mutans* homotetramer. On the other hand, the heterotetramer *R. albus* GlgC/GlgD is 1 order of magnitude less efficient than GlgC/GlgD from the other two *Firmicutes* enzymes. The presence of the GlgD subunits increases the activity and the affinity toward substrates in all the *Firmicutes* heterotetramers. The highest impact of a GlgC/GlgD combination occurs with the less efficient GlgC (*S. mutans*), while the lowest effect is observed in the most efficient GlgC (*G. stearothermophilus*).

Among *Firmicutes*, the *R. albus* GlgC/GlgD is the less efficient ADP-Glc PPase characterized so far. The different kinetic performances of the *Firmicutes* ADP-Glc PPases directly correlate with the ability to complement an *E. coli* mutant deficient for glycogen synthesis. Here we show that the *R. albus* ADP-Glc PPase is sensitive to allosteric regulation. It exhibits different responses depending its quaternary structure (GlgC versus GlgC/GlgD), as similarly described for the *S. mutans* enzyme (8). An

increased sensitivity toward effectors (PEP and Fru-1,6-P_2) occurs in the presence of the GlgD subunit, but the heterotetramer lost the response to activation by Pyr observed for GlgC. Both structures of the enzyme are inhibited by NAD(P)H, with $I_{0.5}$ values that are in the range of 1 to 10 mM. Such an inhibitory effect would be of physiological relevance considering cellular levels of the metabolites and that their redox forms ratio could regulate the enzyme. It is worthy of mention that *Ruminococcus* spp. are organisms that grow in anaerobic environments, following reductive metabolic pathways (including fermentative hydrogen production [31, 32]). In this scenario, carbon metabolism linked to the production and use of NAD(P)H is critical for the cell energetics.

With the idea to understand the dissimilar regulatory properties among *Firmicutes* ADP-Glc PPases better, we conducted a phylogenetic analysis of their GlgC and GlgD proteins. We selected different residues related to allosteric regulation in different ADP-Glc PPases so far characterized and/or in specific regions ascribed to binding regulators (see Fig. S4 in the supplemental material). As shown in Fig. 6, GlgC and GlgD from the *Lactobacillales* group form a clearly separate cluster. Particularly in the case of GlgD, they diverge more than the *Clostridiales* and *Bacillales* groups. The GlgC sequences from *Bacillales*, which contain the catalytic subunit from the unregulated ADP-Glc PPase from *G. stearothermophilus*, are mainly clustered together, with few exceptions. Instead, the *Clostridiales* GlgC split into two clades: one bigger and independent from the other and one smaller and closer to the *Bacillales* branch. The smaller *Clostridiales* group holds the *R. albus* GlgC characterized in this work.

When full sequences were analyzed, both GlgC and GlgD subunits were placed into different branches, resulting in three major clusters grouping *Bacillales*, *Lactobacillales*, and *Clostridiales* (see Fig. 8 in reference 8), which correlates with the phylogenic classification of their species (13, 28). When the phylogenetic tree was constructed with only a fragment sequence, which was selected based on its putative role in regulation (Fig. S4 in the supplemental material), the tree slightly changed (Fig. 6). In this case, the difference between the *Lactobacillales* branch and the rest is more pronounced. Conversely, the difference between *Clostridiales* and *Lactobacillales* is less clear. The divergence in primary structure of the putative regulatory site in *S. mutans* GlgD relates to its more pronounced difference in function. Results herein support the idea that the smaller effects that GlgD from *R. albus* and *G. stearothermophilus* have on their respective GlgC (Table 2) may be explained by their minor divergence in the putative regulatory site. The effect of GlgD on the heterotetramer is an increase of near 500-fold in the Glc-1P catalytic efficiency of *S. mutans* but only 2- to 4-fold in the other groups (Table 2). The effect of GlgD on the ATP catalytic efficiency follows the same trend but at a lower magnitude. The increases in this case are 30, 13.4, and 4.15 for *S. mutans*, *R. albus*, and *S. stearothermophilus*, respectively (data not shown). The fact that the effect on the Glc-1P catalytic efficiency is higher than that of ATP suggests that GlgD induces a conformational change in the heterotetramer that affects the site for those substrates in a different manner. This dramatic change in the catalytic efficiency implies a decrease of the transition state energy (33) in the catalytic GlgC caused by the presence GlgD.

The results presented in this work indicate that the *R. albus* ADP-Glc PPase exhibits distinct regulatory properties, properties that are different from those of other *Firmicutes* enzymes. This work provides relevant structural and functional information to understand the evolutionary history of prokaryotic ADP-Glc PPases. A major conclusion is that allosteric regulation seems to be a rule rather than an exception for the ADP-Glc PPase from *Firmicutes*.

MATERIALS AND METHODS

Chemicals. Restriction enzymes were purchased from Promega. All protein standards, antibiotics, isopropyl-thiogalactoside (IPTG), and oligonucleotides were obtained from Sigma-Aldrich. All other reagents were of the highest quality available.

Bacteria and plasmids. DNA manipulations, molecular biology techniques, and *Escherichia coli* cultures as well as transformations were performed according to standard protocols (34). *E. coli* TOP10 F′ cells (Invitrogen) were used for cloning procedures, while *E. coli* AC70RI-504 (a strain lacking

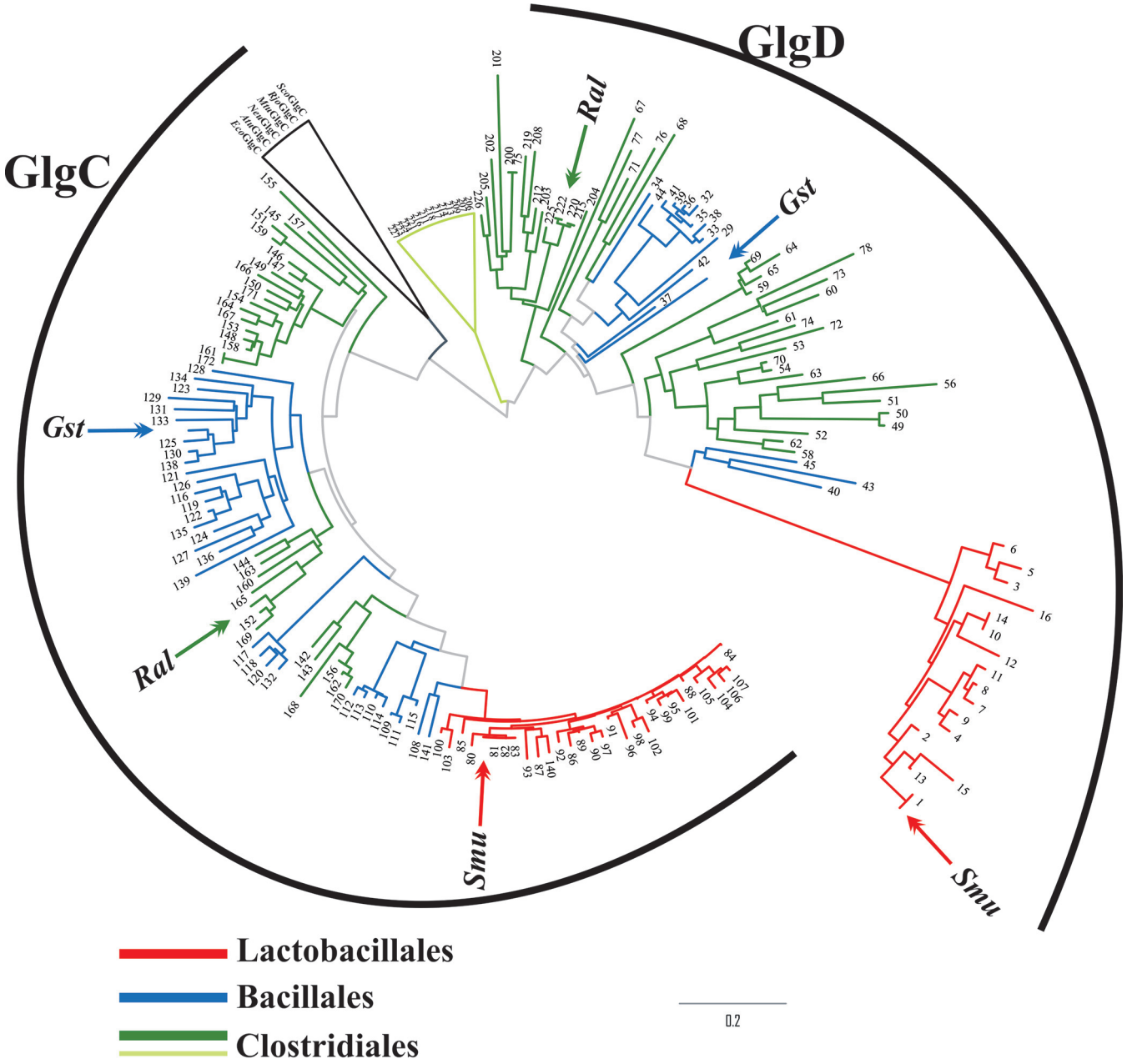

FIG 6 Phylogenetic tree of GlgC and GlgD from *Firmicutes*. Sequences of the GlgC and GlgD polypeptides were collected and the tree was built as described in Materials and Methods. Sequences are numbered with codes indexed in Table S2 in the supplemental material. Different colors represent distinct taxonomy as noted; black indicates sequences taken as reference, and different clusters of *Clostridiales* are indicated by different shades.

endogenous ADP-Glc PPase activity) and *E. coli* BL21(DE3) (Invitrogen) were employed for expression, using plasmids pMAB5, pMAB6, pET24a, pET28c, and pCDFduet (Novagen).

***R. albus glgC* and *glgD* genes.** Genes encoding both ADP-Glc PPase subunits (GlgC and GlgD) from *R. albus* were *de novo* synthetized (Bio Basic Inc.) according to genomic information for *R. albus* 7 (14) in the GenBank database (http://www.ncbi.nlm.nih.gov/nuccore/NC_014833.1). Thus, *R. albus* 7 *glgC* and *glgD* (here *RalglgC* and *RalglgD*, respectively) were designed using *E. coli* codon preference and flanked with NdeI and SacI restriction sites for cloning and expression purposes.

Cloning procedures. The pUC57 plasmids harboring *RalglgC* or *RalglgD* genes were digested with NdeI and SacI. Released genes were separated in a 1% (wt/vol) agarose gel and purified with a Wizard SV Gel & PCR Clean Up kit (Promega). In Fig. S5 in the supplemental material we summarize the general strategies conducted to produce the different conformation of the ADP-Glc PPase from *R. albus*. First, the digested *RalglgC* and *RalglgD* gene were subcloned into pMAB5 (kanamycin resistance) or pMAB6 (spectinomycin resistance) expression vectors, respectively, to obtain pMAB5/*RalglgC* and pMAB6/*RalglgD* constructs. The same strategy was employed to clone the genes into the pET24a and pET28c

TABLE 2 Effect of GlgD on the catalytic efficiency of ADP-Glc PPases from *Firmicutes*

Enzyme form	Parameter	Value for:		
		S. mutans	*R. albus*	*G. stearothermophilus*
GlgC	Glc-1P $S_{0.5}$ (mM)	3.44	0.45	0.14
	k_{cat} (s^{-1})	1.74	2.61	7.58
	$k_{cat}/S_{0.5}$ (s^{-1} mM^{-1})	0.51	5.80	54.1
GlgC/GlgD	Glc-1P $S_{0.5}$ (mM)	0.07	0.27	0.12
	k_{cat} (s^{-1})	17.8	6.05	15.0
	$k_{cat}/S_{0.5}$ (s^{-1} mM^{-1})	254	22.4	125
Relative catalytic efficiency[a]		498	3.86	2.30

[a]Relative catalytic efficiency is the ratio between the catalytic efficiency of GlgC/GlgD over that of the respective GlgC enzyme, i.e., $(k_{cat}/S_{0.5})_{GlgC/GlgD}/(k_{cat}/S_{0.5})_{GlgC}$. The kinetic parameters for the enzymes from *G. stearothermophilus* and *S. mutans* were previously reported in references 7 and 8, respectively.

vectors (both with kanamycin resistance). The former allowed protein production without any tag, whereas the latter rendered proteins with an N-terminal His tag. Afterwards, the *RalglgD* gene was subcloned from plasmid pET28c into the pCDFduet vector (spectinomycin resistance), using NdeI and XhoI (downstream of the SacI site in the pET28 multiple-cloning site) sites, obtaining the pCDFduet/*RalglgD* construction. This construction allowed us to coexpress both GlgC and GlgD subunits by the combination with pET24a/*RalglgC* and pET28C/*RalglgC*, thus obtaining the heteromeric GlgC/GlgD conformation without any tag or with an N-terminal His tag on the GlgC subunit, respectively.

Enzyme expression and purification. *E. coli* AC7OR1-504 cells lacking endogenous ADP-Glc PPase activity were transformed with either pMAB5/*RalglgC* or pMAB6/*RalglgD* to, respectively, produce the GlgC or GlgD protein. In addition, for expression of heteromeric GlgC/GlgD, cells were cotransformed with the pMAB5/*RalglgC* and pMAB6/*RalglgD* compatible plasmids, as reported before (8, 15). All transformed cells were grown in LB medium (10 g/liter of tryptone, 5 g/liter of yeast extract, 10 g/liter of NaCl) at 37°C and 200 rpm, until an optical density at 600 nm (OD_{600}) of ~1.1 was reached. Then recombinant expression of GlgC or GlgD was, respectively, induced (for 16 h at 20°C) with either 0.5 mM IPTG, 0.5 μg/ml of nalidixic acid, or both inducers for the production of the GlgC/GlgD conformation. On the other hand, the GlgC, GlgD, and GlgC/GlgD proteins were overexpressed using *E. coli* BL21(DE3) as a host and transformed with single pET constructions for independent GlgC or GlgD production or combining pCDFduet/*RalglgD* with pET24a/*RalglgC* or pET28C/*RalglgC*, as detailed above. Transformed cells were grown in LB medium at 37°C until the OD_{600} reached 0.6; afterwards, cultures were induced with 0.3 mM IPTG for 16 h at 20°C.

After induction, cells were harvested by centrifugation at 5,000 × *g* for 10 min and stored at −20°C until use. His-tagged proteins were purified by immobilized-metal ion affinity chromatography (IMAC), and all purification steps were performed at 4°C. After resuspension in buffer H (50 mM Tris-HCl [pH 8.0], 300 mM NaCl, 10 mM imidazole, 5% [vol/vol] glycerol), cells were disrupted by sonication (5-s pulse on with intervals of 3-s pulse off for a total time of 15 min on ice) and later centrifuged twice (10 min) at 30,000 × *g*. Supernatants were loaded in a 1-ml His-Trap column (GE Healthcare) previously equilibrated with buffer H. The recombinant proteins were eluted with a 10 to 300 mM imidazole linear gradient in buffer H (50 volumes). Fractions containing the highest activity were pooled, concentrated, and dialyzed against buffer H. The resulting enzyme samples were stored at −80°C until use, remaining fully active for at least 6 months.

On the other hand, cells expressing the proteins without any tag were resuspended in 5 ml of buffer A (50 mM morpholinepropanesulfonic acid [MOPS; pH 8.0], 5 mM $MgCl_2$, 0.1 mM EDTA, and 5% [wt/vol] sucrose) per gram of cells and disrupted by sonication as described above. Supernatants (obtained after two rounds of centrifugation at 30,000 × *g* for 10 min) were loaded onto a 10-ml DEAE-Sepharose fast-flow weak anion exchange column (GE Healthcare) equilibrated with buffer A and eluted with a 0 to 0.5 M NaCl linear gradient (20 column volumes). Fractions containing the highest activity were pooled, supplemented with 20% (vol/vol) glycerol, and stored at −80°C. Under these conditions, the untagged conformation of *R. albus* ADP-Glc PPase samples remained fully active for at least 5 months.

Protein methods. Protein concentration was determined according to the method of Bradford (35) using bovine serum albumin (BSA) as a standard. Recombinant proteins and purification fractions were defined by sodium dodecyl sulfate-polyacrylamide gel electrophoresis (SDS-PAGE) according to the method of Laemmli (36). Gels were loaded with 5 to 50 μg of protein per well and stained with Coomassie brilliant blue. Western blotting was performed after standard techniques (34). Briefly, proteins in the gel were blotted onto polyvinylidene difluoride (PVDF) membranes using a Mini-PROTEAN II (Bio-Rad) apparatus. The membranes were blocked 2 h at room temperature and subsequently incubated overnight with primary antibodies (anti-GlgC or anti-GlgD) at 4°C. After intensive washing, membranes were incubated with Alexa Fluor 647–goat anti-rabbit IgG(H+L) (Invitrogen) for 1 h at 25°C. Detection was carried out by scanning membranes at 650 nm with the Typhoon 9400 (GE Healthcare) equipment. Antibodies raised against GlgC or GlgD from *G. stearothermophilus* were produced according to established methods (37) and were used as previously reported (8). Both antibodies were purified from rabbit sera by consecutive precipitation steps with ammonium sulfate 50% and 33% (twice) saturation

solutions, resuspended in TBS buffer (Tris-HCl [pH 8.0], 150 mM NaCl) and desalted using an ultrafiltration device with a 30-kDa cutoff (Amicon).

Iodine staining assay. Experiments were carried out according to previous reports (8, 38). Briefly, transformed *E. coli* AC70R1-504 cells harboring pMAB5/*RalglgC*, pMAB6/*RalglgD*, or both were inoculated onto 3 ml of LB medium and grown at 37°C until they reached an OD_{600} of ~0.8. Then protein expression was induced with 0.5 mM IPTG for 3 h at 20°C. Then 2% (wt/vol) glucose was added and the incubation was extended for 1 h at the same temperature. An aliquot of 0.1 ml was withdrawn and centrifuged at 10,000 × *g* for 5 min. The supernatant was removed and cells were washed with 50 mM phosphate buffer (pH 7.0). After centrifugation (5,000 × *g* for 5 min), a compact pellet was allocated to the bottom of the tube. Then the tube was turned upside down and an iodine crystal positioned in the cap to stain the cell pellet with iodine vapor (38). Alternatively, glycogen was visualized after staining liquid growth media with 500 μl of Lugol solution and stained pellets were photographed after centrifugation (5,000 × *g* for 5 min).

Extraction and quantification of polysaccharides. An alkali treatment protocol was conducted for polysaccharide extraction, as described previously (12, 39–41). Samples of 10 ml from *E. coli* AC70RI-504 cells transformed with pMAB5/*RalglgC*, pMAB6/*RalglgD*, or both plasmids together were pelleted, washed with ice-cold water, resuspended to an OD_{600} of 5.0, and boiled for 5 min. Then 0.3 ml 30% (wt/vol) KOH per ml of cell suspension was added and samples were boiled for 90 min. After cooling and neutralization with acetic acid, polysaccharides were precipitated with 3 volumes of 97% (vol/vol) ethanol at 0°C. Suspensions were centrifuged at 20,000 × *g*, and then polysaccharides were dissolved in 0.1 ml of water. Thirty-microliter aliquots were digested with 2 U of amyloglucosidase (EC 3.2.1.3; Sigma-Aldrich) from *Aspergillus niger* in 100 mM acetate buffer (pH 4.5) for 2 h at 55°C, in a final volume of 100 μl. Glucose was determined by a specific glucose oxidase method (42). The amount of measured glucose was considered the glycogen content and was expressed related to the total amount of pelleted cells.

Molecular mass determination. Protein molecular mass was determined by gel filtration using a Tricorn 5/200 column (GE Healthcare) loaded with Superdex G200 resin (GE Healthcare). A gel filtration calibration kit (high molecular weight; GE Healthcare) with protein standards including thyroglobulin (669 kDa), ferritin (440 kDa), aldolase (158 kDa), conalbumin (75 kDa), and ovalbumin (44 kDa) was used. The column void volume was determined using a dextran blue loading solution (Promega, Fitchburg, WI).

Enzyme activity assays. ADP-Glc PPase activity was determined at 37°C in ADP-Glc synthesis direction by following P_i formation after hydrolysis of PP_i by inorganic pyrophosphatase, using a highly sensitive colorimetric method (43). Reaction mixtures contained (unless otherwise specified) 50 mM MOPS (pH 8.0), 10 mM $MgCl_2$, 2.0 mM ATP, 0.2 mg/ml of bovine serum albumin, 0.5 U/ml of yeast inorganic pyrophosphatase, and a proper enzyme dilution. Assays were initiated by addition of 1.5 mM Glc-1P in a total volume of 50 μl. Reaction mixtures were incubated for 10 min at 37°C and terminated when malachite green reactive was added. The complex formed with the released P_i was measured at 630 nm in an enzyme-linked immunosorbent assay (ELISA) EMax detector (Molecular Devices).

One unit of activity is defined as the amount of enzyme catalyzing the formation of 1 μmol of product per min under the conditions described above in each case.

Calculation of kinetic constants. Saturation curves were determined by assaying enzyme activity at different concentrations of the variable substrate or effector and saturating levels of the others. Experimental data were plotted as enzyme activity (units per milligram) versus substrate (or effector) concentration (millimolar), and kinetic constants were determined by fitting the data to the Hill equation as described elsewhere (5). Fitting was performed with the Levenberg-Marquardt nonlinear least-squares algorithm provided by the computer program Origin 8.0. Hill plots were used to calculate the Hill coefficient (n_H), the maximal velocity (V_{max}), and the kinetic constants that correspond to the activator, substrate, or inhibitor concentrations giving 50% of the maximal activation ($A_{0.5}$), velocity ($S_{0.5}$), or inhibition ($I_{0.5}$). All kinetic constants are the means from at least three independent sets of data, which were reproducible within a range of ±10%.

Phylogenetic analysis. Amino acid sequences of different GlgC and GlgD polypeptides belonging to ADP-Glc PPases from *Firmicutes* were downloaded from the NCBI database (http://www.ncbi.nlm.nih.gov/). They were filtered to remove duplicates and near duplicates (i.e., mutants and strains from same species). After a preliminary alignment, constructed using the ClustalW multiple-sequence alignment server (http://www.genome.jp/tools/clustalw/) (44), sequences with a wrong annotation or that were truncated were also eliminated manually. Sequences having less than 30% identity to any other and did not have all the characterized critical motifs, and catalytic residues were discarded. After this, sequences were chosen to represent most of the taxonomic groups from *Firmicutes*. Sequences were classified into different groups using taxonomic data provided by the NCBI as depicted in Table S2 in the supplemental material. Once selected, the sequences were aligned using the program T-Coffee (45). A manual inspection was performed to guarantee that all known conserved regions (i.e., catalytic or binding associated residues) were properly aligned. Then we chose specific sequence regions to build the tree and the rest were deleted. The selection was based on the domains and/or residues related to allosteric regulation according to previous reports or structural data (see Fig. S4 in the supplemental material). Trees were constructed by maximum likelihood with the program PhyML (46) incorporated into Seaview. Confidence coefficients for the tree branches were obtained and plotted. Finally, the tree was prepared with the FigTree 1.3 program (http://tree.bio.ed.ac.uk/) (47).

Homology modeling. Modeling of the GlgC subunit from the *R. albus* ADP-Glc PPase was performed using the program Modeler 9.19. The structure was modeled using the structure of the homologous

enzymes from *A. tumefaciens* (PDB code 3BRK) and that from *E. coli* in complex with Fru-1,6-P_2 (PDB code 5L6S). The reliability of the model was evaluated using the program Verify 3D (48).

SUPPLEMENTAL MATERIAL

Supplemental material for this article may be found at https://doi.org/10.1128/JB.00172-18.

SUPPLEMENTAL FILE 1, PDF file, 1.4 MB.

ACKNOWLEDGMENTS

This work was supported by grants from ANPCyT (PICT 2014 3362 and PICT 2015 0634 to M.D.A.D. and PICT 2015 1767 to A.A.I.), UNL (CAID 2016 to A.A.I.), and NSF (MCB 1616851 to M.A.B.). M.D.A.D. and A.A.I. are members of the Research Career from CONICET. A.E.C. has a doctoral fellowship from CONICET.

REFERENCES

1. Preiss J. 2009. Glycogen biosynthesis, p 145–158. *In* Schaechter M (ed), Encyclopedia of microbiology. Academic Press (Elsevier), Cambridge, MA.
2. Iglesias AA, Preiss J. 1992. Bacterial glycogen and plant starch biosynthesis. Biochem Educ 20:196–203. https://doi.org/10.1016/0307-4412(92)90191-N.
3. Ballicora MA, Iglesias AA, Preiss J. 2003. ADP-glucose pyrophosphorylase, a regulatory enzyme for bacterial glycogen synthesis. Microbiol Mol Biol Rev 67:213–225. https://doi.org/10.1128/MMBR.67.2.213-225.2003.
4. Ballicora MA, Iglesias AA, Preiss J. 2004. ADP-glucose pyrophosphorylase: a regulatory enzyme for plant starch synthesis. Photosynth Res 79:1–24. https://doi.org/10.1023/B:PRES.0000011916.67519.58.
5. Ballicora MA, Erben ED, Yazaki T, Bertolo AL, Demonte AM, Schmidt JR, Aleanzi M, Bejar CM, Figueroa CM, Fusari CM, Iglesias AA, Preiss J. 2007. Identification of regions critically affecting kinetics and allosteric regulation of the Escherichia coli ADP-glucose pyrophosphorylase by modeling and pentapeptide-scanning mutagenesis. J Bacteriol 189:5325–5333. https://doi.org/10.1128/JB.00481-07.
6. Kiel JA, Boels JM, Beldman G, Venema G. 1994. Glycogen in Bacillus subtilis: molecular characterization of an operon encoding enzymes involved in glycogen biosynthesis and degradation. Mol Microbiol 11:203–218. https://doi.org/10.1111/j.1365-2958.1994.tb00301.x.
7. Takata H, Takaha T, Okada S, Takagi M, Imanaka T. 1997. Characterization of a gene cluster for glycogen biosynthesis and a heterotetrameric ADP-glucose pyrophosphorylase from Bacillus stearothermophilus. J Bacteriol 179:4689–4698. https://doi.org/10.1128/jb.179.15.4689-4698.1997.
8. Asención Diez MD, Demonte AM, Guerrero SA, Ballicora MA, Iglesias AA. 2013. The ADP-glucose pyrophosphorylase from Streptococcus mutans provides evidence for the regulation of polysaccharide biosynthesis in Firmicutes. Mol Microbiol 90:1011–1027. https://doi.org/10.1111/mmi.12413.
9. Asención Diez MD, Demonte AM, Syson K, Arias DG, Gorelik A, Guerrero SA, Bornemann S, Iglesias AA. 2015. Allosteric regulation of the partitioning of glucose-1-phosphate between glycogen and trehalose biosynthesis in Mycobacterium tuberculosis. Biochim Biophys Acta 1850:13–21. https://doi.org/10.1016/j.bbagen.2014.09.023.
10. Asención Diez MD, Peiru S, Demonte AM, Gramajo H, Iglesias AA. 2012. Characterization of recombinant UDP- and ADP-glucose pyrophosphorylases and glycogen synthase to elucidate glucose-1-phosphate partitioning into oligo- and polysaccharides in Streptomyces coelicolor. J Bacteriol 194:1485–1493. https://doi.org/10.1128/JB.06377-11.
11. Cereijo AE, Asencion Diez MD, Davila Costa JS, Alvarez HM, Iglesias AA. 2016. On the kinetic and allosteric regulatory properties of the ADP-glucose pyrophosphorylase from Rhodococcus jostii: an approach to evaluate glycogen metabolism in oleaginous bacteria. Front Microbiol 7:830. https://doi.org/10.3389/fmicb.2016.00830.
12. Demonte AM, Asencion Diez MD, Naleway C, Iglesias AA, Ballicora MA. 2017. Monofluorophosphate blocks internal polysaccharide synthesis in Streptococcus mutans. PLoS One 12:e0170483. https://doi.org/10.1371/journal.pone.0170483.
13. Zhang W, Lu Z. 2015. Phylogenomic evaluation of members above the species level within the phylum Firmicutes based on conserved proteins. Environ Microbiol Rep 7:273–281. https://doi.org/10.1111/1758-2229.12241.
14. Suen G, Stevenson DM, Bruce DC, Chertkov O, Copeland A, Cheng JF, Detter C, Detter JC, Goodwin LA, Han CS, Hauser LJ, Ivanova NN, Kyrpides NC, Land ML, Lapidus A, Lucas S, Ovchinnikova G, Pitluck S, Tapia R, Woyke T, Boyum J, Mead D, Weimer PJ. 2011. Complete genome of the cellulolytic ruminal bacterium Ruminococcus albus 7. J Bacteriol 193:5574–5575. https://doi.org/10.1128/JB.05621-11.
15. Iglesias AA, Barry GF, Meyer C, Bloksberg L, Nakata PA, Greene T, Laughlin MJ, Okita TW, Kishore GM, Preiss J. 1993. Expression of the potato tuber ADP-glucose pyrophosphorylase in Escherichia coli. J Biol Chem 268:1081–1086.
16. Ballicora MA, Sesma JI, Iglesias AA, Preiss J. 2002. Characterization of chimeric ADPglucose pyrophosphorylases of Escherichia coli and Agrobacterium tumefaciens. Importance of the C-terminus on the selectivity for allosteric regulators. Biochemistry 41:9431–9437.
17. Ebrecht AC, Solamen L, Hill BL, Iglesias AA, Olsen KW, Ballicora MA. 2017. Allosteric control of substrate specificity of the Escherichia coli ADP-glucose pyrophosphorylase. Front Chem 5:41. https://doi.org/10.3389/fchem.2017.00041.
18. Cornish-Bowden A, Cardenas ML. 2010. Specificity of non-Michaelis-Menten enzymes: necessary information for analyzing metabolic pathways. J Phys Chem B 114:16209–16213. https://doi.org/10.1021/jp106968p.
19. Segel IH. 1975. Enzyme kinetics: behavior and analysis of rapid equilibrium and steady-state enzyme systems. John Wiley & Sons, New York, NY.
20. Gómez Casati DF, Aon MA, Iglesias AA. 2000. Kinetic and structural analysis of the ultrasensitive behaviour of cyanobacterial ADP-glucose pyrophosphorylase. Biochem J 350(Part 1):139–147. https://doi.org/10.1042/bj3500139.
21. Asención Diez MD, Aleanzi MC, Iglesias AA, Ballicora MA. 2014. A novel dual allosteric activation mechanism of Escherichia coli ADP-glucose pyrophosphorylase: the role of pyruvate. PLoS One 9:e103888. https://doi.org/10.1371/journal.pone.0103888.
22. Christopherson MR, Dawson JA, Stevenson DM, Cunningham AC, Bramhacharya S, Weimer PJ, Kendziorski C, Suen G. 2014. Unique aspects of fiber degradation by the ruminal ethanologen Ruminococcus albus 7 revealed by physiological and transcriptomic analysis. BMC Genomics 15:1066. https://doi.org/10.1186/1471-2164-15-1066.
23. Thurston B, Dawson KA, Strobel HJ. 1994. Pentose utilization by the ruminal bacterium Ruminococcus albus. Appl Environ Microbiol 60:1087–1092.
24. Lee SS, Ha JK, Cheng KJ. 2000. Relative contributions of bacteria, protozoa, and fungi to in vitro degradation of orchard grass cell walls and their interactions. Appl Environ Microbiol 66:3807–3813. https://doi.org/10.1128/AEM.66.9.3807-3813.2000.
25. Flint HJ, Scott KP, Duncan SH, Louis P, Forano E. 2012. Microbial degradation of complex carbohydrates in the gut. Gut Microbes 3:289–306. https://doi.org/10.4161/gmic.19897.
26. Kang S, Denman SE, Morrison M, Yu Z, Dore J, Leclerc M, McSweeney CS. 2010. Dysbiosis of fecal microbiota in Crohn's disease patients as revealed by a custom phylogenetic microarray. Inflamm Bowel Dis 16:2034–2042. https://doi.org/10.1002/ibd.21319.

27. Park J, Lee J, Yeom Z, Heo D, Lim Y-H. 2017. Neuroprotective effect of Ruminococcus albus on oxidatively stressed SH-SY5Y cells and animals. Sci Rep 7:14520. https://doi.org/10.1038/s41598-017-15163-5.
28. Rainey FA, Janssen PH. 1995. Phylogenetic analysis by 16S ribosomal DNA sequence comparison reveals two unrelated groups of species within the genus Ruminococcus. FEMS Microbiol Lett 129:69–73.
29. Desvaux M, Guedon E, Petitdemange H. 2000. Cellulose catabolism by Clostridium cellulolyticum growing in batch culture on defined medium. Appl Environ Microbiol 66:2461–2470. https://doi.org/10.1128/AEM.66.6.2461-2470.2000.
30. Cheng KJ, Brown RG, Costerton JW. 1977. Characterization of a cytoplasmic reserve glucan from Ruminococcus albus. Appl Environ Microbiol 33:718–724.
31. Ntaikou I, Gavala HN, Kornaros M, Lyberatos G. 2008. Hydrogen production from sugars and sweet sorghum biomass using Ruminococcus albus. Int J Hydrogen Energy 33:1153–1163. https://doi.org/10.1016/j.ijhydene.2007.10.053.
32. Ntaikou I, Gavala HN, Lyberatos G. 2009. Modeling of fermentative hydrogen production from the bacterium Ruminococcus albus: definition of metabolism and kinetics during growth on glucose. Int J Hydrogen Energy 34:3697–3709. https://doi.org/10.1016/j.ijhydene.2009.02.057.
33. Fersht A. 1999. Structure and mechanism in protein science: a guide to enzyme catalysis and protein folding. WH Freeman, New York, NY.
34. Sambrook J, Russell DW. 2001. Molecular cloning: a laboratory manual, 3rd ed. Cold Spring Harbor Laboratory Press, Cold Spring Harbor, NY.
35. Bradford MM. 1976. A rapid and sensitive method for the quantitation of microgram quantities of protein utilizing the principle of protein-dye binding. Anal Biochem 72:248–254. https://doi.org/10.1016/0003-2697(76)90527-3.
36. Laemmli UK. 1970. Cleavage of structural proteins during the assembly of the head of bacteriophage T4. Nature 227:680–685. https://doi.org/10.1038/227680a0.
37. Vaitukaitis JL. 1981. Production of antisera with small doses of immunogen: multiple intradermal injections. Methods Enzymol 73:46–52. https://doi.org/10.1016/0076-6879(81)73055-6.
38. Demonte AM, Asencion Diez MD, Guerrero SA, Ballicora MA, Iglesias AA. 2014. Iodine staining of Escherichia coli expressing genes involved in the synthesis of bacterial glycogen. Bio Protoc 4(17):e1224.
39. DiPersio JR, Mattingly SJ, Higgins ML, Shockman GD. 1974. Measurement of intracellular iodophilic polysaccharide in two cariogenic strains of Streptococcus mutans by cytochemical and chemical methods. Infect Immun 10:597–604.
40. Elbein AD, Mitchell M. 1973. Levels of glycogen and trehalose in Mycobacterium smegmatis and the purification and properties of the glycogen synthetase. J Bacteriol 113:863–873.
41. Hernández MA, Alvarez HM. 2010. Glycogen formation by Rhodococcus species and the effect of inhibition of lipid biosynthesis on glycogen accumulation in Rhodococcus opacus PD630. FEMS Microbiol Lett 312:93–99. https://doi.org/10.1111/j.1574-6968.2010.02108.x.
42. Trinder P. 1969. Determination of blood glucose using an oxidase-peroxidase system with a non-carcinogenic chromogen. J Clin Pathol 22:158–161. https://doi.org/10.1136/jcp.22.2.158.
43. Fusari C, Demonte AM, Figueroa CM, Aleanzi M, Iglesias AA. 2006. A colorimetric method for the assay of ADP-glucose pyrophosphorylase. Anal Biochem 352:145–147. https://doi.org/10.1016/j.ab.2006.01.024.
44. Jeanmougin F, Thompson JD, Gouy M, Higgins DG, Gibson TJ. 1998. Multiple sequence alignment with Clustal X. Trends Biochem Sci 23:403–405.
45. Notredame C, Higgins DG, Heringa J. 2000. T-Coffee: a novel method for fast and accurate multiple sequence alignment. J Mol Biol 302:205–217. https://doi.org/10.1006/jmbi.2000.4042.
46. Gouy M, Guindon S, Gascuel O. 2010. SeaView version 4: a multiplatform graphical user interface for sequence alignment and phylogenetic tree building. Mol Biol Evol 27:221–224. https://doi.org/10.1093/molbev/msp259.
47. Guindon S, Gascuel O. 2003. A simple, fast, and accurate algorithm to estimate large phylogenies by maximum likelihood. Syst Biol 52:696–704. https://doi.org/10.1080/10635150390235520.
48. Lüthy R, Bowie JU, Eisenberg D. 1992. Assessment of protein models with three-dimensional profiles. Nature 356:83–85. https://doi.org/10.1038/356083a0.